Optical Diffraction-Free Patterns Induced by a Discrete Translational Transport

P. L. Ramazza, S. Ducci,* and F. T. Arecchi*

Istituto Nazionale di Ottica, Largo Enrico Fermi, 6, I50125, Florence, Italy
and INFM, Unita' di Firenze
(Received 8 June 1998)

We report the formation of spatial structures induced by a spatial offset in a two-dimensional nonlinear optical interferometer in which diffractive effects are absent. The observed patterns arise from the destabilization of wide, continuous bands in the Fourier spectrum. The selection of these bands is shown to be determined by the interplay between the amount of spatial offset and the strength of the diffusion in the nonlinear optical material.   [S0031-9007(98)07536-X]

Dynamical instabilities leading to the formation of spatial structures in extended systems driven out of thermodynamical equilibrium [1] have been shown to occur extensively in the realm of nonlinear optics [2–4]. Among the systems in which optical pattern formation has been studied we recall lasers, nonlinear interferometers, and systems formed by a nonlinear medium with diffractive feedback. In most of these systems the selection of the spatial frequencies that bifurcate, resulting in formation of spatial structures, is largely ruled by diffraction. As a consequence, a field of wavelength λ propagating within a nonlinear optical system, including a free propagation length l, forms patterns at a "diffractive" spatial frequency $f_0 \simeq (\lambda l)^{-1/2}$, or at a discrete set of frequencies simply related to f_0 [5].

Pattern formation in the absence of diffraction has been studied in optical systems with a rotation in the feedback loop [6,7]. The suppression of diffractive effects is obtained by adopting an image-forming configuration within a nonlinear interferometer. We stress that, being diffraction peculiar to wave fields, its suppression leads to a dynamics that loses its specificity of being an "optical" one. Its identifying characteristics are spatial extension, nonlinearity, and nonlocal interactions.

In this Letter, we study the formation of optical patterns without diffraction when nonlocal interactions are introduced in the system via a spatial offset Δx. Systems with continuous transport given, e.g., by a drift velocity, resulting in the breaking of the translational symmetry and in the onset of convective and absolute pattern forming instabilities, have recently been studied in several physical systems [8–10].

The experimental setup consists of a liquid crystal light valve (LCLV) with optical feedback (Fig. 1). The LCLV operates as a defocusing Kerr medium working in reflection. The optical beam reflected from the valve's front face undergoes a phase retardation u proportional to the light intensity fed to the valve's rear face. Because of the anisotropy of the liquid crystal molecules, however, the phase retardation affects only the electric field component along the projection $e_\parallel$ of the liquid crystal director on the LCLV plane.

In our experiments, a plane light beam from an Ar^+ laser operating at 514 nm impinges on the front of the LCLV linearly polarized at an angle θ_1 with respect to $e_\parallel$. The reflected light is fed back to the rear face of the LCLV after passing through a polarizer with the transmissive axis oriented at an angle θ_2 with respect to $e_\parallel$. This produces on the rear side of the LCLV an optical field given by the superposition of the component polarized along $e_\parallel$, which has acquired the phase retardation u, and of the component polarized orthogonally to $e_\parallel$. A couple of lenses in the feedback loop provides a one-to-one image of the LCLV front face onto a coherent fiber bundle that, in turn, relays this image to the back face of the LCLV. In this way any effect due to diffractive free propagation in the system is eliminated.

Furthermore, we introduce a nonlocal interaction by means of a transverse displacement of the optical wavefront in the feedback loop by an amount Δx. The displacement is experimentally achieved by the use of a micrometric screw connected to the input end of the fiber bundle, allowing variations of Δx with a resolution of 5 μm. In these conditions, the phase induced by the
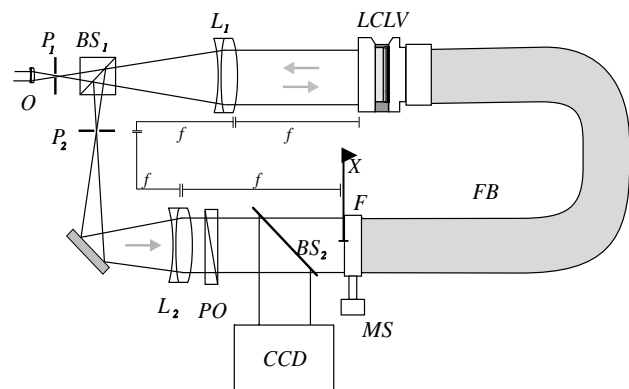
FIG. 1.   Experimental setup. O: microscope objective; P_1, P_2: pinholes; BS_1, BS_2: beam splitters; LCLV: liquid crystal light valve; L_1, L_2: lenses of focal length f; FB: fiber bundle; PO: polarizer; X: direction of feedback displacement; MS: micrometric screw; CCD: videocamera. The $4f$ configuration of the feedback loop provides a one-to-one imaging of the LCLV front plane on the F plane.

liquid crystals on the light polarized along $e_\parallel$ obeys the equation [11]

$$\tau \frac{\partial u}{\partial t} = -u(x, y, t) + l_d^2 \nabla_\perp^2 u(x, y, t)$$
$$- aI_0\{1 + \gamma \cos[u(x + \Delta x, y, t)$$
$$+ u_0(V_0, \nu)]\}, \qquad (1)$$

where I_0 is the input intensity, $\tau \simeq 100$ ms and $l_d \simeq 30$ μm are, respectively, the response time and the diffusion length of the LCLV, (x, y) are the coordinates in the plane transverse to the propagation direction z, $\nabla_\perp^2$ is the Laplacian operator in the (x, y) plane, and α is positive (defocusing medium) and is comprehensive of both the optical losses of the feedback loop and the responsivity of the LCLV. The constant phase $u_0(V_0, \nu)$ sets the working point of the LCLV and is controlled by means of the ac voltage of frequency ν and amplitude V_0 rms applied to it. Throughout the experiments reported here we kept fixed $\nu = 4$ KHz, $V_0 = 9$ V resulting in $u_0 \simeq 4\pi$. The modulation term $\gamma = \frac{\cos^2(\theta_1 - \theta_2) - \cos^2(\theta_1 + \theta_2)}{\cos^2(\theta_1 - \theta_2) + \cos^2(\theta_1 + \theta_2)}$ [11] has the value of 0.978, having fixed $\theta_1 = 48°$ and $\theta_2 = 48°$.

Equation (1) for $\Delta x = 0$ is known to give rise to optical multistability among different homogeneous stationary solutions for sufficiently high values of I_0. In the experiment reported here, we choose low values of I_0, so that the system always remains in the lowest branch of stability for $\Delta x = 0$. Even though the homogeneous state is stable for $\Delta x = 0$, a nonlocal interaction due to $\Delta x \neq 0$ can destabilize this state. Indeed, any spatial perturbation of period $2\Delta x$ in the direction of the offset will provide a negative feedback but applied with a spatial phase shift of π, thus providing a growing deviation from equilibrium. This is the space counterpart of a time lag in a feedback amplifier. Preliminary evidence of pattern formation in these conditions has been presented in [6], though both qualitative and quantitative analyses are lacking.

This mechanism breaks the stability of the homogeneous state inducing patterned states in the system. In Fig. 2 we report the intensity patterns with their corresponding far field patterns obtained by holding the input

intensity $I_0 = 150$ μW/cm^2 and gradually increasing Δx. No patterns are observed for $\Delta x \leq 100$ μm. For small values of Δx the structures observed are roll-like, with a spatial frequency decreasing for increasing Δx, as can be expected from the above discussion. For high values of Δx a continuous band of wave vectors is excited, resulting in patterns of increasing richness in the near field.

Some important aspects of these phenomena are already explained by a linear stability analysis of Eq. (1). The temporal growth rate of the Fourier mode of spatial frequency $\vec{q} = (q_x, q_y)$ has real and imaginary parts, $\lambda_{\vec{q}}$ and $\omega_{\vec{q}}$, given by

$$\tau \lambda_q = -1 - l_d^2(q_x^2 + q_y^2) - \beta I_0 \cos(q_x \Delta x), \qquad (2)$$

and

$$\tau \omega_q = -\beta I_0 \sin(q_x \Delta x), \qquad (3)$$

with $\beta \equiv -\alpha \gamma \sin(\tilde{u} + u_0)$. Here $\tilde{u}$ denotes the homogeneous stationary solution of Eq. (1) for $\Delta x = 0$, the linear stability of which is considered. In the experimental conditions considered here, β is always positive, thus ensuring the stability of the homogeneous stationary solution $\tilde{u}$ for $\Delta x = 0$.

From Eq. (2) $\lambda_q > 0$ requires $\cos(\tilde{q}_x \Delta x) < 0$. Furthermore, the modes with maximum growth rate are given by

$$2l_d^2 \tilde{q}_x - \beta I_0 \Delta x \sin(\tilde{q}_x \Delta x) = 0, \qquad (4)$$

$$\tilde{q}_y = 0. \qquad (5)$$

Equation (4) has $\tilde{q}_x$ solutions corresponding to the intersections of a straight line of slope $2l_d^2/\Delta x \beta I_0$ with $\sin(\tilde{q}_x \Delta x)$. For $\Delta x \gg l_d$ the straight line is very close to the horizontal axis; therefore, the sine function is intersected close to its zeros. Expanding around $\tilde{q}_x \Delta x = n\pi$ (n odd to comply with the previous condition of negative cosine) yields the approximate solution $\tilde{q}_x \simeq n\pi/\Delta x$. Therefore, for large Δx, the most unstable mode is the one having a spatial frequency equal to the inverse of the spatial shift, as can be expected from our qualitative

Δx=130 μm Δx=320 μm Δx=500 μm Δx=660 μm Δx=820 μm Δx=980 μm
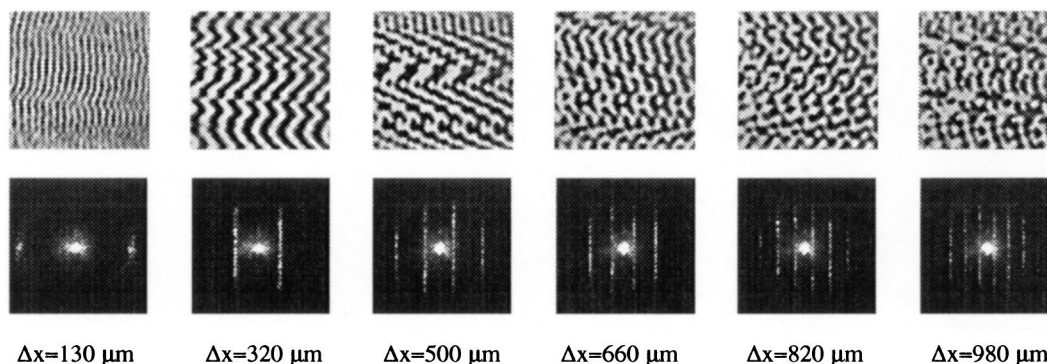
FIG. 2. Experimental patterns for fixed $I_0 = 150$ μW/cm^2 and increasing Δx. Top: near field. Bottom: far field, corresponding to the Fourier spectrum.
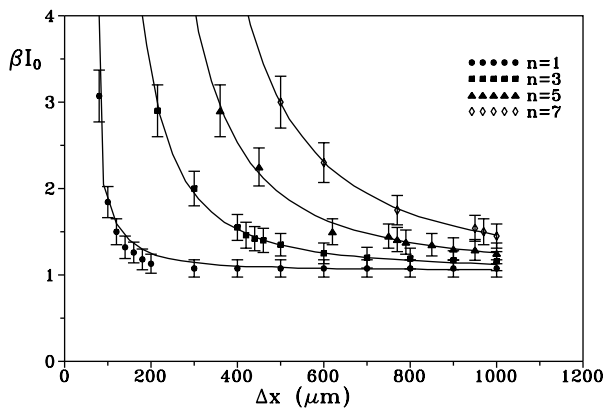
FIG. 3. Marginal stability curve, βI_0 vs Δx. Continuous line: theory. Dots: experiment. The fit between theory and experiment is obtained for $\beta = 0.012$ cm$^2/\mu$W. The different curves are relative to excited bands of different order n (see text).

discussion on the instability mechanism. Relevant deviations from this result occur instead for $\Delta x \lesssim l_d$.

The threshold condition for the destabilization of the uniform steady state is obtained from Eq. (2) and Eqs. (4) and (5) as

$$\beta I_{0\text{-th}} = \frac{1 + l_d^2 \tilde{q}_x^2}{\cos(\tilde{q}_x \Delta x)}. \qquad (6)$$

The numerical solution of Eqs. (2) and (3) gives the marginal stability curve $\beta I_{0\text{-th}}(\Delta x)$ and the frequency selection curve $q_x(\Delta x)$ which agree well with experimental measurements, as shown in Figs. 3 and 4.

A nonzero imaginary part ω_q of the eigenvalue implies that mode q has a phase velocity $v_q = \omega_q/q$. From Eq. (3) it is to be expected that the observed pattern drifts at a velocity proportional to $\sin(q_x \Delta x)$. This term is very close to 0 for $\Delta x \gg l_d$, and indeed no drift is observed in these conditions. For small values of Δx ($\Delta x \lesssim 200$ μm), the observed intensity pattern actually drifts at a velocity of the order of 100 μm/s that decreases for increasing values of Δx.

In order to compare the prediction of the linear stability analysis with the experimental observation reported in Fig. 2, we investigate the behavior of the system when it is driven slightly above threshold. In this case, a broadening $\Delta \vec{q}$ of the unstable band is to be expected. In Fig. 4 we report the unstable q_x and q_y bands vs Δx for $\epsilon = \frac{I_0 - I_{\text{th}}}{I_{\text{th}}} = 0.42$, numerically calculated from Eqs. (2) and (6), together with their experimental counterparts. Along q_x, the bands are centered around a Δx-dependent finite wave number [Fig. 4(a)]. Along q_y, for each Δx the band of excited wave numbers ranges from 0 to a finite value [Fig. 4(b)]. For graphic clarity, in Fig. 4(b) we plot only the extrema of the experimentally excited bands, instead of all of the destabilized wave numbers, as we do in Fig. 4(a). Notice that, due to the symmetries $q_x \to -q_x$, $q_y \to -q_y$ of Eq. (2), the whole set of unstable wave numbers is given by the ones represented
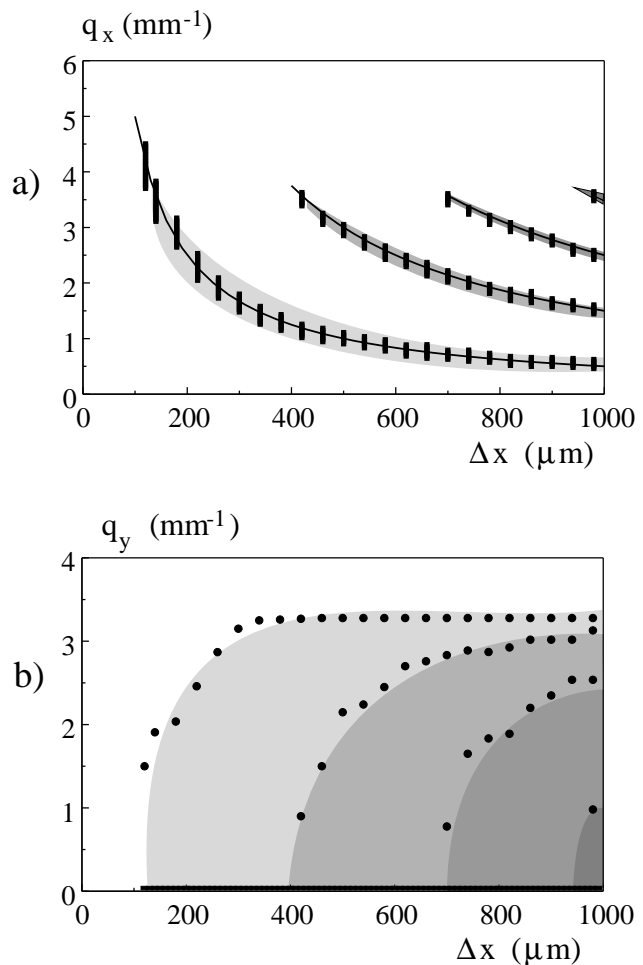
FIG. 4. Spatial frequency selection curves in the $(\Delta x, q_x)$ and $(\Delta x, q_y)$ planes. (a) The theory provides the continous lines at threshold and the shadowed regions are unstable stripes for $\epsilon \equiv (I_0 - I_{\text{th}})/I_{\text{th}} = 0.42$. Light to dark gray correspond, respectively, to $n = 1$, 3, 5, and 7 in the asymptotic relation $q_x \simeq n\pi/\Delta x$. The vertical bars correspond to experimentally excited wave numbers, for $\epsilon = 0.42$. (b) For each n value and for $\epsilon = 0.42$, the theory provides a whole range of spatial frequencies from $q_y = 0$ to the maximum corresponding to the boundary of each gray region. The gray code is as in (a). The bold line $q_y = 0$ and the points represent, respectively, the minimum and maximum values of experimentally excited wave numbers for $\epsilon = 0.48$.

in Figs. 4(a) and 4(b), plus their symmetrical ones having negative signs of q_x and q_y.

The amount of the band broadening along q_x and q_y can be evaluated by expanding $\lambda(q, I_0)$ in a Taylor series around the threshold point $(q_{\text{th}}, I_{0\text{-th}})$ for each Δx and then imposing $\lambda(q, I_0) > 0$. This condition gives $|\Delta q_i| < \sqrt{-\beta \Delta I_0/R_i}$, where $i = x, y, \Delta I_0 \equiv I_0 - I_{0\text{-th}}$, and we defined the curvatures of the curve $\lambda(\vec{q})$ around its maximum as $R_i \equiv \frac{1}{2} \frac{\partial^2 \lambda}{\partial q_i^2}|_{q_{\text{th}}, I_{0\text{-th}}}$. The expression of these curvatures reads

$$R_x = -l_d^2 + \frac{1}{2} \beta I_{0\text{-th}} (\Delta x)^2 \cos(\tilde{q}_x \Delta x), \qquad (7)$$
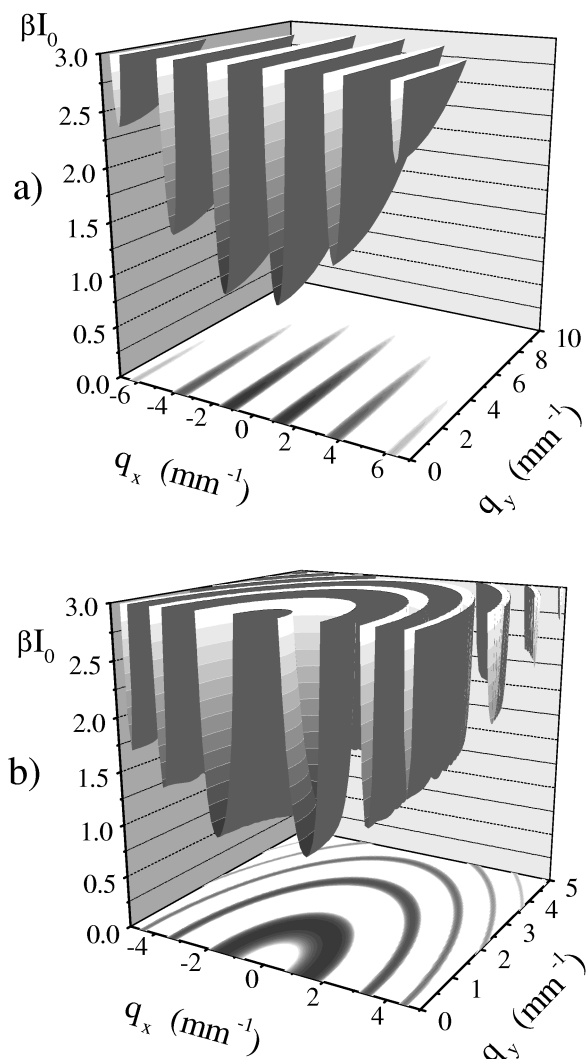
FIG. 5. Marginal stability curves for the problem here considered with $\Delta x = 500$ μm (a) and for a Kerr medium with optical feedback (b). The diffusion length is $l_d = 30$ μm in both cases. The diffractive length $(\lambda l)^{1/2}$ for the Kerr medium with feedback is 450 μm. In the (q_x, q_y) plane it is represented as a projection of the marginal stability curves, with the same gray scale used for the three-dimensional structure.

$$R_y = -l_d^2. \tag{8}$$

For fixed pump intensity I_0, it can be seen that the curvature along q_x is determined both by a diffusion term and by a term that specifically takes into account the nonlocal interaction. Since $\cos(\tilde{q}_x \Delta x) < 0$, this term always tends to increase the absolute value of R_x, resulting in a Δx-dependent limitation to the broadening along q_x as experimentally observed. Along q_y, however, the only limiting factor to the bandwidth broadening is diffusion. For large values of Δx, where $I_{0\text{-th}}$ is nearly constant, the broadening of the bands follows the dependence of R_x and R_y on Δx. For small values of Δx, correction to this behavior due to the dependence of $I_{0\text{-th}}$ on Δx (Fig. 3) is observed.

The experimentally observed asymmetry of the broadening along q_x and q_y is well reproduced by the numerics. The very large value of this asymmetry, due to the fact that broadening along q_y is limited only by diffusion, is in contrast with many other pattern forming instabilities occurring both in optics and in other fields. In order to elucidate this point, we report in Fig. 5 a comparison between the marginal stability curves for the system discussed here and for a pattern forming system consisting of a defocusing Kerr slice with purely diffractive feedback and without spatial shift [5]. In this latter case, the diffractive scale $(\lambda l)^{1/2}$ determines the width of the excited bands in any spatial direction. This length is much larger than l_d in typical operating conditions, where the narrowness of the diffractive bands is compared to the diffusion-limited band that is present along q_y in the case presented here.

In conclusion, we have presented evidence of optical pattern formation due to a spatial shift in the absence of diffraction. The experimental occurrence of continuous bands of unstable spatial frequencies with exceptionally large width, as compared with other pattern forming systems, has been explained in terms of the different interplay of nonlocal shift and diffusion in two orthogonal directions.

*Also at Dept. of Physics, University of Florence, Florence, Italy.
[1] M. Cross and P. C. Hohenberg, Rev. Mod. Phys. **65**, 851 (1993).
[2] Special issue on Nonlinear Optical Structures, Patterns, Chaos, edited by L. A. Lugiato, Chaos Solitons Fractals **4**(8/9), (1994), and references therein.
[3] F. T. Arecchi, Physica (Amsterdam) **41D**, 297 (1995), and references therein.
[4] P. L. Ramazza, E. Pampaloni, S. Residori, and F. T. Arecchi, Physica (Amsterdam) **96D**, 259 (1996), and references therein.
[5] W. J. Firth, J. Mod. Opt. **37**, 151 (1990); G. D'Alessandro and W. J. Firth, Phys. Rev. Lett. **66**, 2597 (1991).
[6] S. A. Akhmanov *et al.*, J. Opt. Soc. Am. B **9**, 78 (1992).
[7] P. L. Ramazza, S. Residori, E. Pampaloni, and A. V. Larichev, Phys. Rev. A **53**, 400 (1996).
[8] A. Couarion and J. M. Chomaz, Phys. Rev. Lett. **79**, 2666 (1997).
[9] K. L. Babcock, G. Ahlers, and D. S. Cannell, Phys. Rev. Lett. **67**, 3388 (1991).
[10] M. Santagiustina, P. Colet, M. San Miquel, and D. Walgraef, Phys. Rev. Lett. **79**, 3633 (1997).
[11] R. Neubecker, G. L. Oppo, B. Thuering, and T. Tschudi, Phys. Rev. A **52**, 791 (1995).